

## GAMMA-RAY EMISSION IN GALAXY CLUSTER FROM DARK MATTER ANNIHILATION

C. Combet<sup>1</sup>

**Abstract.** Clusters of galaxies are potentially important targets for indirect detection of dark matter (DM) in  $\gamma$ -rays, be it from DM annihilation or decay. Here we summarise the results of three recent papers, where we reassessed DM indirect detection prospects in massive halos making use of the recently-released Meta-Catalogue of X-ray Clusters. In particular, we find a stacking strategy to be marginally beneficial for space-borne  $\gamma$ -ray observatories while completely redhibitory for ground-based instruments.

Keywords: Galaxies:clusters:general, Dark matter, Gamma-rays:general

### 1 Introduction

The annihilation (or decay) of dark matter (DM) particles into  $\gamma$ -rays has been flagged as one of the most promising channels for indirect detection. While the Galactic centre is the most obvious target (Silk & Bloemen 1987), its large astrophysical  $\gamma$ -ray background makes identification of an exotic signal challenging (e.g., Aharonian et al. 2004). A good alternative lies with dwarf spheroidal galaxies (dSphs), which are background-free, relatively close by and with DM density profiles that can be constrained from their internal kinematics (e.g., Evans et al. 2004; Walker et al. 2011; Charbonnier et al. 2011; Ackermann et al. 2011).

Due to their huge DM content, clusters of galaxies have also been investigated for indirect detection studies. Although strong constraints have already been derived from X-ray and gravitational lensing studies on the DM distribution in clusters (Pointecouteau et al. 2005; Vikhlinin et al. 2006; Buote et al. 2007; Shan et al. 2010; Pastor Mira et al. 2011; Etori et al. 2011), obtaining a clear picture of their inner DM distribution is still a challenging task. The standard approach is then to assume NFW (Navarro, Frenk & White 1997) or Einasto (e.g., Merritt et al. 2006) profiles for these objects. Doing so, Fornax, Coma or Perseus have been identified as the best targets for DM emission (Jeltema et al. 2009; Pinzke et al. 2011) when using parameters from 170 clusters of the HIFLUGCS catalogue (Reiprich & Böhringer 2002; Chen et al. 2007).

In three recent papers (Combet et al. 2012; Maurin et al. 2012; Nezri et al. 2012) we make use of the new Meta-Catalogue of X-ray detected Clusters (1743 objects), MCXC (Piffaretti et al. 2011), to i) provide a new ranking of best targets using the MCXC cluster parameters, ii) quantify the improvement of a stacking approach over a single-source analysis and iii) find new directions to discriminate between astrophysical and exotic signals. In this proceeding, we only summarise the first two items in the case of DM annihilation.

### 2 Modelling DM annihilation $\gamma$ -ray emission

The  $\gamma$ -ray flux  $\Phi_\gamma$  from dark matter annihilations ( $\text{cm}^{-2} \text{s}^{-1} \text{sr}^{-1} \text{GeV}^{-1}$ ) received on Earth in a solid angle  $\Delta\Omega$  is generically written as

$$\frac{d\Phi_\gamma}{dE_\gamma} = \frac{1}{4\pi} \frac{\langle\sigma_{\text{ann}}v\rangle}{2m_\chi^2} \cdot \frac{dN_\gamma}{dE_\gamma} \times J(\Delta\Omega), \quad (2.1)$$

where  $m_\chi$  is the particle mass,  $\langle\sigma_{\text{ann}}v\rangle$  is the velocity-averaged annihilation cross section and  $dN_\gamma/dE_\gamma$  is the energy spectrum of annihilation products. The  $dN_\gamma/dE_\gamma$  term depends on the particle physics model and

---

<sup>1</sup> Laboratoire de Physique Subatomique et de Cosmologie, Université Joseph Fourier Grenoble 1/CNRS/IN2P3/INPG, 53 avenue des Martyrs, 38026 Grenoble, France

is discussed here. Instead, we focus solely on the so-called astrophysics factor  $J$  which corresponds to the integration along the line of sight of the dark matter density squared,

$$J(\Delta\Omega) = \int_{\Delta\Omega} \int \rho^2(l, \Omega) dl d\Omega. \quad (2.2)$$

The latter is computed with the CLUMPY code (Charbonnier et al. 2012), that has been designed to perform this integral in a variety of setups and with large versatility (Milky-way DM halo or external halo, user-defined dark matter profiles, different concentration prescriptions, inclusion of substructures, integration angle, etc.).

For the DM halo smooth profile, we use an NFW (Navarro, Frenk & White 1997)

$$\rho(r) = \frac{\rho_s}{\left(\frac{r}{r_s}\right) \left(1 + \frac{r}{r_s}\right)^2}, \quad (2.3)$$

where  $r_s$  is the scale radius and  $\rho_s$  is the normalisation. We note that Einasto profiles (Merritt et al. 2006) give slightly more ‘signal’ than NFW halos, making our conclusions on detectability conservative.

Cold DM N-body simulations show a high level of clumpiness in the DM distribution (e.g., Diemand et al. 2007; Springel et al. 2008). These substructures boost the signal in the outer parts of the DM halos and should be properly taken into account. The substructure modelling goes as follows: i) the mass distribution is  $dN_{\text{subs}}/dM \propto M^{-1.9}$  with a mass fraction  $f = 10\%$  in substructures (Springel et al. 2008), a minimal and maximal mass of  $10^{-6} M_{\odot}$  and  $10^{-2} M_{\text{cluster}}$  respectively, and the Bullock et al. (2001) concentration (down to the minimal mass); ii) the substructure spatial distribution  $dN_{\text{subs}}/dV$  follows the host halo smooth profile. With this as our reference configuration, we obtain boost factors of  $\sim 10 - 20$  for the MCXC galaxy clusters. Note that the value of the boost can vary by one or two orders of magnitude depending on the modelling (see sec. 3.4 and figure 4 of Nezri et al. 2012) but that our chosen configuration gives a rather conservative estimate.

### 3 Results

The 1743 clusters of the MCXC catalogue are processed using the above modelling. The normalisation of each cluster profile (i.e.  $\rho_s$  and  $r_s$ ) is obtained using the  $M_{500}$  and  $R_{500}$ <sup>1</sup> provided in the catalogue.

The symbols in figure 1 give the  $J$ -factor of all the MCXC clusters as a function of their angle  $\phi$  to the Galactic centre, for integration angles  $\alpha_{\text{int}} = 0.1^\circ$  (left panel) and  $\alpha_{\text{int}} = 0.5^\circ$  (right panel). The brightest halos are identified with specific symbols. The solid black line corresponds to the total (smooth and substructures) exotic background of the Milky-way halo, peaking at the Galactic centre. The number of halos lying below the Galactic background depends on the integration angle, the contrast  $J_{\text{cluster}}/J_{\text{Gal}}$  increasing as the integration angle is decreased because of the concentrated emission in clusters. Online material of Nezri et al. (2012) gathers the  $J$ -values of all MCXC clusters which can readily be used by others. Our new ranking of ‘best’ targets differs slightly from results based on the HIFLUGCS catalogue (Jeltema et al. 2009; Pinzke et al. 2011) because of the different gas density model used in the MCXC; the results are nonetheless in overall agreement (see Appendix B in Nezri et al. 2012).

The shear number of clusters with significant  $J$ -factors (fig. 1, left) had us considering stacking as a viable option to improve the limit of indirect detection. The  $\log J - \log N$  histogram (not shown here) has a slope of  $\sim -2$ , which is a first indication of the potential of stacking: in the absence of background noise, stacking ten times more objects increases the flux by a factor 100. This is however a too naive view and the signal-to-noise ratio must be considered before any conclusion can be reached.

The left panel in figure 2 shows the evolution of the  $S/N$  ratio when stacking cluster signals (in decreasing order of  $J$ ) for several integration angles (colours). The signal-to-noise ratio goes through a maximum corresponding to a given number of stacked clusters. Stacking more objects increases the noise faster than the signal and becomes pointless. The optimal number of objects to stack increases with decreasing integration angle, once again because of the very centrally-located emission in cluster of galaxies.

Finally, realistic instrumental responses and observational strategies must be considered. For an all-sky  $\gamma$ -ray instrument as Fermi-LAT, all sources are naturally observed the same amount of time. Conversely, for a given granted observation time at a ground-based facility – like the future Cerenkov Telescope Array (CTA) –, a

<sup>1</sup>The radius  $R_{500}$  is defined as the radius within which the average density is 500 times the critical density of the Universe (at a given redshift), and  $M_{500}$  is the mass within  $R_{500}$ .

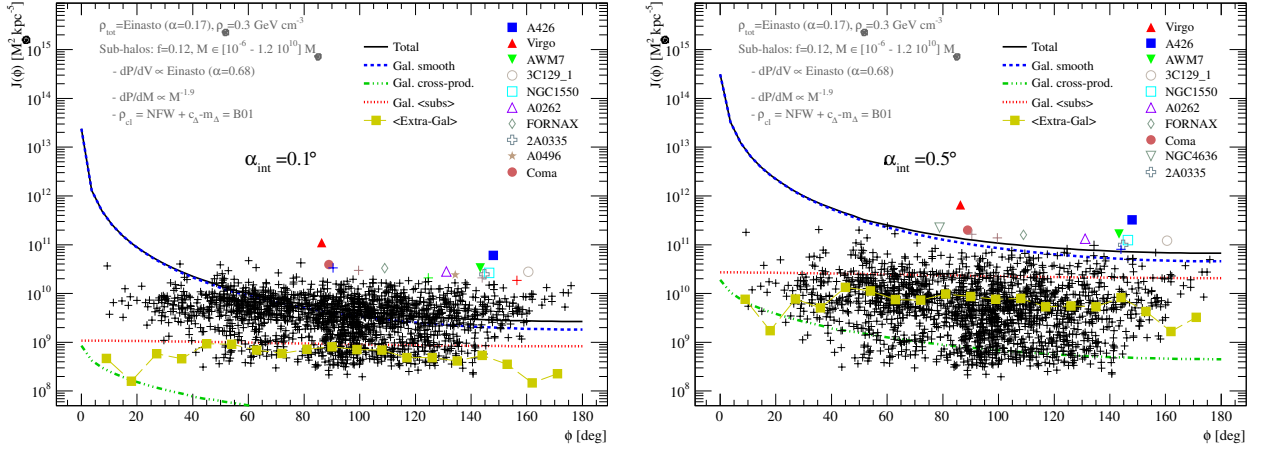


**Fig. 1.** Computed  $J$ -factors for the MCXC sources (the 10 highest-contrast clusters are highlighted, the remaining are shown with a ‘+’ symbol) vs Galactic DM background (total is the sum of smooth, sub-halos, and cross-product [see details in Charbonnier et al. 2012]). The yellow filled square symbols are evaluated from the cumulative of the cluster signal in different  $\phi$  bins: this can be interpreted as a lower limit for the extra-galactic DM annihilation signal. **Left panel:** integration angle  $\alpha_{\text{int}} = 0.1^\circ$ . **Right panel:**  $\alpha_{\text{int}} = 0.5^\circ$ .

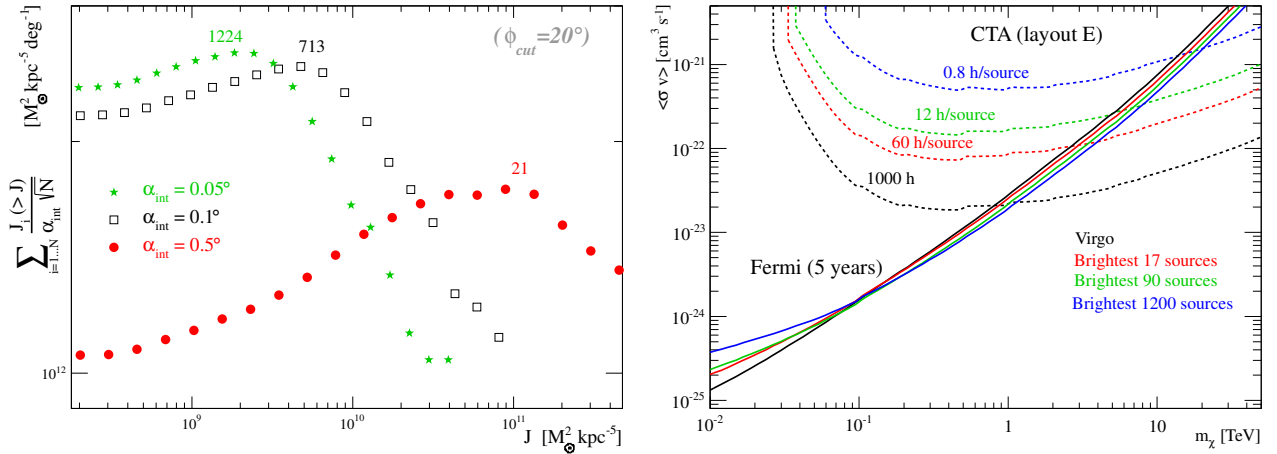


**Fig. 2.** **Left panel:**  $\sum_i J_i(>J)/\alpha_{\text{int}}\sqrt{N}$  (proportional to the cumulative signal-to-noise for a fixed integration angle) as a function of  $J$  for the same integration angles. **Right panel:** The  $5\sigma$  sensitivity of Fermi-LAT (5 years exposure) (solid curves) and CTA (1000 hours total exposure) for stack sizes of the optimum number of sources for a  $0.1^\circ$  (1200) (blue),  $0.5^\circ$  (90) (green) and  $1^\circ$  (17) (red) PSF. Virgo alone is shown in black. For CTA the 1000 hour exposure is divided equally over the number of sources in the stack.

choice must be made between observing one source for the all duration, or attempting to stack several objects, hence dividing-up the observation time. The summary of these considerations is given in fig. 2 (right). This shows in the mass-cross section plane (see eq.(2.1)) the limits that can be achieved using either 5 years of Fermi-LAT data, or 1000 h with CTA. Different colours correspond to stacking different number of objects (with the appropriate integration angle to make stacking optimum for that number of object).

For Fermi-LAT, the stacking strategy yields a marginal improvement (about  $\times 2$ ) above  $M_\chi \sim 0.1$  TeV. Below this value, the instrument is in background-limited regime, with poor angular resolution: stacking actually worsens the limit at low energies. For ground-based instruments like CTA, the observation time must be divided up among sources which leads to much less constraining exclusion limits: for ground-based instruments, the best strategy is to look at the supposedly brightest object for as long as possible.

We mentioned in the introduction that dwarf spheroidal galaxies are also very interesting targets for indirect detection. In recent works (Charbonnier et al. 2011; Walker et al. 2011), we have studied the detectability of

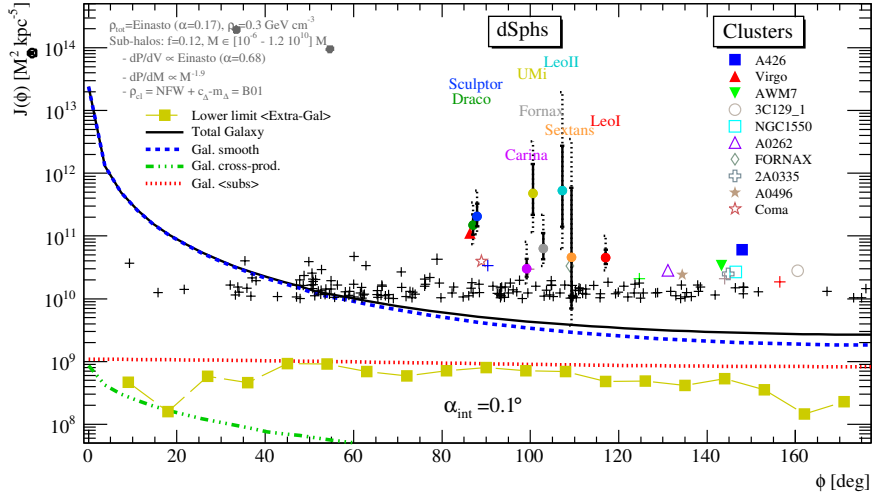


**Fig. 3.** Same as fig. 1 (left). Symbols with errors bars correspond to  $J$ -factors of dSph as evaluated by Charbonnier et al. (2011). Symbols without error bars correspond to the clusters of this study (not all 1743 clusters have been plotted here.).

these objects with Fermi-LAT and CTA. In figure 3, we finally compare the  $J$ -factors of the MCXC galaxy clusters to that of dSph galaxies. The brightest clusters have similar  $J$  values to the faintest dSph galaxies. Despite large error bars, some of the latter (like Leo II or Ursa Minor) are significantly brighter, making them *a priori* more favourable targets. The lack of cosmic ray induced  $\gamma$ -ray emission in dSph galaxies is another argument in their favour. As discussed in Maurin et al. (2012), this astrophysical signal is present in galaxy clusters and makes the identification of an exotic signal a more difficult task. Note however that the large uncertainty linked to the substructure boost in clusters prevent making too strong a conclusion.

## 4 Conclusions

We have evaluated the  $J$ -factor of DM annihilation for the 1743 galaxy clusters of the MCXC catalogue. The values we find are in overall agreement with previous studies but differ because of the more robust gas modelling used in the MCXC. In studying the benefit of stacking, we find it is marginally worthwhile for all-sky instruments but completely redhibitory for ground-based telescopes. A benefit of stacking lies nonetheless in the fact that it is a way to wash out the large modelling uncertainties of the dark matter halo in galaxy clusters. In comparing the detection prospect in galaxy clusters to that of dSph galaxies, we conclude that dSph remain a safer option given the clean  $\gamma$ -ray environment they host and the stronger observational constraints that can be put on their dark matter profiles.

## References

- Ackermann, M. et al. 2011, Physical Review Letters, 107, 241302  
 Aharonian, F. et al. 2004, A&A, 425, L13  
 Bullock, J. S., Kolatt, T. S., Sigad, Y., et al. 2001, MNRAS, 321, 559  
 Buote, D. A., Gastaldello, F., Humphrey, P. J., et al. 2007, ApJ, 664, 123  
 Charbonnier, A., Combet, C., Daniel, M., et al. 2011, MNRAS, 418, 1526  
 Charbonnier, A., Combet, C., & Maurin, D. 2012, Computer Physics Communications, 183, 656  
 Chen, Y., Reiprich, T. H., Böhringer, H., Ikebe, Y., & Zhang, Y.-Y. 2007, A&A, 466, 805  
 Combet, C., Maurin, D., Nezri, E., et al. 2012, Phys. Rev. D, 85, 063517  
 Diemand, J., Kuhlen, M., & Madau, P. 2007, ApJ, 657, 262  
 Ettori, S., Gastaldello, F., Leccardi, A., et al. 2011, A&A, 526, C1  
 Evans, N. W., Ferrer, F., & Sarkar, S. 2004, Phys. Rev., D69, 123501  
 Jeltema, T. E., Kehayias, J., & Profumo, S. 2009, Phys. Rev. D, 80, 023005

- Maurin, D., Combet, C., Nezri, E., & Pointecouteau, E. 2012, ArXiv e-prints: 1203.1166, A&A accepted
- Merritt, D., Graham, A. W., Moore, B., Diemand, J., & Terzić, B. 2006, AJ, 132, 2685
- Navarro, Frenk & White. 1997, ApJ, 490, 493
- Nezri, E., White, R., Combet, C., et al. 2012, MNRAS, 425, 477
- Pastor Mira, E., Hilbert, S., Hartlap, J., & Schneider, P. 2011, A&A, 531, A169
- Piffaretti, R., Arnaud, M., Pratt, G. W., Pointecouteau, E., & Melin, J.-B. 2011, A&A, 534, A109
- Pinzke, A., Pfrommer, C., & Bergström, L. 2011, Phys. Rev. D, 84, 123509
- Pointecouteau, E., Arnaud, M., & Pratt, G. W. 2005, A&A, 435, 1
- Reiprich, T. H. & Böhringer, H. 2002, ApJ, 567, 716
- Shan, H., Qin, B., Fort, B., et al. 2010, MNRAS, 406, 1134
- Silk, J. & Bloemen, H. 1987, ApJ, 313, L47
- Springel, V., Wang, J., Vogelsberger, M., et al. 2008, MNRAS, 391, 1685
- Vikhlinin, A., Kravtsov, A., Forman, W., et al. 2006, ApJ, 640, 691
- Walker, M. G., Combet, C., Hinton, J. A., Maurin, D., & Wilkinson, M. I. 2011, ApJ, 733, L46